

OPTIMIZATION OF LIGAMENT PARAMETERS ON A SUBJECT-SPECIFIC  
COMPUTATIONAL HUMAN KNEE MODEL IN A DYNAMIC KNEE SIMULATOR USING  
DESIGN OF EXPERIMENTS

A THESIS IN  
Mechanical Engineering

Presented to the Faculty of the University  
of Missouri-Kansas City in partial fulfillment of  
the requirements for the degree

MASTER OF SCIENCE

by

PAUL M. WILSON

B.S., University of Missouri-Kansas City, 2007

Kansas City, Missouri

2011

© 2011

PAUL MICHAEL WILSON

ALL RIGHTS RESERVED

OPTIMIZATION OF LIGAMENT PARAMETERS ON A SUBJECT-SPECIFIC  
COMPUTATIONAL HUMAN KNEE MODEL IN A DYNAMIC KNEE SIMULATOR USING  
DESIGN OF EXPERIMENTS

Paul Wilson, Candidate for the Master of Science Degree

University of Missouri-Kansas City, 2011

ABSTRACT

The objective of this study was to optimize ligament parameters used in a dynamic three-dimensional subject-specific computational knee model. The parameters of interest are the zero load length ( $L_0$ ), stiffness ( $k$ ) and the strain level where the force length relationship of the ligament goes from the nonlinear “toe” region to the linear region ( $\varepsilon_l$ ). Experimental testing was performed at the University of Kansas Experimental Joint Biomechanics Research Laboratory (Lawrence, Kansas) in the Kansas Knee Simulator (KKS) under various loading profiles while the kinematics of the knee was recorded. A model of the knee in the KKS was created using previously validated modeling techniques. The experimental and model simulation kinematics for a ten second walk cycle were compared in a two level partial factorial design and a three level full factorial design and the ligament parameters were optimized based on the kinematic RMS error. The resulting parameter values are 80 % of the experimentally derived zero load length values, 99.71% of the published ligament stiffness values, and 100% of the published  $\varepsilon_l$ . These values are reasonable, and are validated by the stiffness values from the optimization closely matching published values for each ligament’s stiffness.

## APPROVAL PAGE

The faculty listed below, appointed by the Dean of the School of Computing and Engineering have examined a thesis titled “Optimization of Ligament Parameters on a Subject-Specific Computational Human Knee Model in a Dynamic Knee Simulator Using Design of Experiments” presented by Paul M. Wilson, candidate for the Master of Science degree, and certify that their opinion is worthy of acceptance.

### Supervisory Committee

Trent Guess, Ph.D.  
Assistant Professor  
School of Computing and Engineering

Ganesh Thiagarajan, Ph.D.  
Assistant Professor  
School of Computing and Engineering

Gregory W. King, Ph.D.  
Assistant Professor  
School of Computing and Engineering

## CONTENTS

ABSTRACT.....	iii
ILLUSTRATIONS .....	vi
TABLES .....	vii
CHAPTER	
1. INTRODUCTION .....	1
2. LITERATURE REVIEW OF COMPUTATIONAL KNEE MODEL LIGAMENTS AND THEIR PARAMETERS.....	3
3. MATERIALS AND METHODS.....	8
4. RESULTS .....	32
5. CONCLUSION.....	48
6. DISCUSSION .....	50
Appendix.....	53
REFERENCES .....	58
VITA .....	60

## ILLUSTRATIONS

Figure	Page
1: MRI Tracing and Model Creation Using Slicer 3.4.....	11
2: KKS Alignment Points .....	13
3: Femur Rigid Body Marker "Femur_Marker" Relative to Femur Model in KKS.....	14
4: KN05 Aligned in KKS.....	15
5: Ligaments in Model (LCL and PCL).....	15
6: Ligaments in Model (ACL and MCL).....	16
7: Example of Spline Creation Spreadsheet.....	17
8: Spline Creation Spreadsheet with Piecewise Equation Shown .....	19
9: Ligament Force Splines Based on 80% of Experimental Zero Strain Length.....	20
10: Simulink Control Plant with PID Parameters .....	21
11: Simulink Control Plant Position Feedback.....	22

## TABLES

Table	Page
1: Ligament Stiffness Parameters (Blankevoort et al., 1991) .....	18
2: Two-level Fractional Factorial Design Parameters .....	23
3: Two Level Partial Factorial Design .....	32
4: Tibia RMS Errors.....	33
5: Patella RMS Errors .....	34
6: Effects Calculated from the Tibia Coordinate System .....	34
7: Effects Calculated from the Patella Coordinate System .....	35
8: Predicted Tibia RMS Errors .....	36
9: Predicted Patella RMS Errors .....	36
10: Tibia Prediction Errors.....	36
11: Patella Prediction Errors .....	37
12: Tibia Coefficients of Determination .....	38
13: Patella Coefficients of Determination.....	38
14: Design Matrix .....	40
15: Tibia RMS Error .....	42
16: Patella RMS Error.....	43
17: Quadriceps Force RMS Error .....	44
18: Profile 1: Significant Effects Highlighted in Yellow.....	45
19: Profile 2: Significant Effects Highlighted in Yellow.....	45
20: Profile 3: Significant Effects Highlighted in Yellow.....	46
21: Profile 4: Significant Effects Highlighted in Yellow.....	46

22: Profile 5: Significant Effects Highlighted in Yellow.....	46
23: Profile 6: Significant Effects Highlighted in Yellow.....	46
24: Profile 7: Significant Effects Highlighted in Yellow.....	47



## CHAPTER 1

### INTRODUCTION

Computational subject specific knee modeling is important in predicting the reactions of a human knee under various loading conditions. The modeling techniques can help predict and prevent injury, and further understanding of the internal loads of the knee. Since it is impossible to measure ligament parameters directly in an intact knee, it is important to gain an understanding of the values of ligament parameters and to develop techniques for predicting these values.

The knee consists of the tibiofemoral joint (TFJ) and the patellofemoral joint (PFJ). The ligaments in the knee connect the tibia and the femur and consist of the anterior cruciate ligament (ACL), posterior cruciate ligament (PCL), medial collateral ligament (MCL) and lateral collateral ligament (LCL). The ligaments of the knee keep the condyles of the femur in place on the tibial plateau, and guide the knee during motion. Forces in the ligaments are important to predicting injuries in the knee such as tearing.

Anatomically correct ligament parameters are significant to evaluating and predicting ligament related injuries, such as torn ACL, in living subjects, and one of the first steps in using dynamic simulations is to identify methods for preventing injuries. In 2006 there were over one hundred thousand ACL reconstruction surgeries in the United States (Lyman et al. 2009). ACL injuries are common among athletes. With appropriate ligament parameters and computational modeling techniques, ACL injuries can be predicted, analyzed, and possibly prevented by developing training programs that involve appropriate muscle use.

The presented thesis is concerned with improving ligament representation in subject specific computational knee models by providing optimization techniques for determining the

ligament parameters in an intact knee. Design of experiments (DOE) methods were used to optimize the system's ligament parameters based on the experimental results. This thesis work is the first step in developing standard ligament parameters based on knee laxity tests. A knee laxity test is commonly used to test for ligament tearing, and is non-intrusive to the knee being tested.

## CHAPTER 2

### LITERATURE REVIEW OF COMPUTATIONAL KNEE MODEL LIGAMENTS AND THEIR PARAMETERS

Mathematical knee models are of great interest for predicting forces and pressures inside the knee that cannot be measured. Anatomical models require an accurate description of the underlying structures. The ligaments play an important role in the motion and structure of the knee, and therefore are important to the anatomical models.

Knee joint stability is achieved by a combination of bony geometry and soft tissue constraints. Ligamentous restraints guide and restrict the motion of the knee. Ligaments are a biological composite of a ground substance matrix reinforced by collagen and elastin. Ligaments include elongated, interconnected fibroblast cells in their midsubstance, and more rounded cells found near their bony insertions. Water makes up about two-thirds of the weight of a normal ligament, and 70 to 80% of the remaining weight is made up of fibrillar protein collagen (Wiess et al. 2001).

There are many ways to represent ligaments in mathematical models of joints, like the knee. The one-dimensional discrete element representation of a ligament is typically modeled as a simple linear or nonlinear spring, and allows the entire representation of the ligament to be reduced to a load-elongation relationship. Two-dimensional representations of a ligament are able to predict quantities such as soft tissue stress, which is not possible with a one dimensional model. In order to accurately model ligament stresses and interactions with surrounding tissue, a three-dimensional continuum representation of a ligament's structure is required. One and two-dimensional ligament models are insufficient for describing and predicting the complex three-

dimensional behavior of ligaments, but three-dimensional models are not often used due to difficulties associated with their formulation and complexity (Wiess et al. 2001).

An anatomical dynamic model of the knee was validated using the Kansas Knee Simulator (KKS) (Weimer, 2007). The model included both the tibio-femoral joint (TFJ) and the Patello-femoral joint (PFJ). Weimer modeled the KKS and the anatomical knee using MSC.ADAMS. The model was used to validate a subject-specific anatomical knee model in the KKS and to develop techniques for accurately modeling soft tissue contact, ligament behavior, and basic ligament and tendon bone wrapping. Along with the Weimer 2007 model, four other anatomical dynamic knee models stand out: Caruntu and Hefzy 2004, Piazza and Delp 2001, Abdel-Rahman and Hefzy 1998, and Guess and Maletsky 2004.

In Guess and Maletsky 2004, no ligaments were modeled; instead the computational model of a total knee prosthetic used the contacts between tibio-femoral geometries to provide constraint to the out-of-sagittal-plane loading from the KKS. The KKS and prosthetic geometries were developed in MSC.ADAMS. The model was used to produce inputs to the controllable axes of the KKS for reproduction of experimental loading and motion.

In Weimer 2007, the cruciate ligaments were broken into two bundles each, while the collateral ligaments were represented by a single element each. Blankevoort et al. 1991 also used two bundles for each of the cruciate ligaments, but used three bundles for each of the collateral ligaments. Piazza and Delp 2001 represented two bundle models of both the collateral ligaments, but did not represent the cruciate ligaments as a prosthesis was being modeled. In Caruntu and Hefzy 2004 and Abdel-Rahman and Hefzy 1998, the LCL was represented with a single bundle, while the MCL was represented with three bundles, and the cruciates were represented with two bundles each. Chhabra et al. 2006 reports that the ACL is made up of two

bundles, the anteromedial bundle (aACL) and the posterolateral bundle (pACL). Similarly, DeFrate et al. 2008 describes the PCL as consisting of two bundles, the anterolateral bundle (aPCL) and the posteromedial bundle (pPCL). The collateral ligaments, however, are typically broken into three bundles each, as reported by Park et al. 2006.

Blankevoort et al. 1991, Caruntu and Hefzy 2004, Piazza and Delp 2001, and Abdel-Rahman and Hefzy 1998 use a continuous piecewise function to calculate the resultant ligament forces from knee motion. Weimer 2007 uses the same equation, but creates splines to represent the force length relationship of the ligaments. The continuous piecewise function describes the zero compressive force when ligaments are slack, the non-linear toe region of ligaments at low force, and the linear region of the ligaments at high force values. Piazza and Delp 2001 didn't represent the linear region of the ligament function as it was anticipated that collateral ligament strains would be small. Values for stiffness and zero load length were computed from estimates of ligament strain in extension which were derived from literature. Blankevoort et al. 1991 and Abdel-Rahman and Hefzy 1998 use published stiffness parameters and zero load lengths. Weimer 2007 uses published stiffness parameters for the ligaments, but subject specific zero strain length.

The insertion location of the ligaments on the femur and the tibia is an important consideration as well. Caruntu and Hefzy 2004 and Abdel-Rahman and Hefzy 1998 used published data to define the ligamentous insertion points. Piazza and Delp 2001 chose ligament attachment sites that produced normal ligament length patterns during prescribed tibio-femoral motions. Blankevoort et al. 1991 used roentgenstereophotogrammetry to obtain subject specific ligament insertion information while the Weimer 2007 model used subject specific information, obtained by probing the dissected cadaver knee joint, to place the ligament elements. Park et al.

2006 used Magnetic Resonance Images (MRI) to locate the insertion sites for the collateral ligaments. Chhabra et al. 2006 reports the insertion location of the ACL bundles based on cadaver studies.

Bertozzi et al. 2008 studied a cruciate ligament's sensitivity to reference length and the elastic modulus during drawer test simulation. Both the ACL and PCL were represented by 25 linear fibers. Model results were compared to experimental results to gain sensitivity data for the laxity and the anterior and posterior stiffness of the ACL and PCL based on changes to the reference length and elastic modulus. The nonlinear mechanical behavior of each ligament is modeled by progressive recruitment of fibers. The elastic modulus is used to mechanically characterize the cruciates, but additional parameters were obtained from literature, as it was not possible to obtain them from the selected subject. They found that underestimations of the reference length produced bigger anterior/posterior forces due to faster recruitment of the fibers, whereas underestimation of the reference length produced smaller anterior/posterior forces. Laxity and anterior/posterior stiffness estimations values were not very sensitive to changes in the reference length. Anterior and posterior stiffness's were the parameters most sensitive to variations in the elastic modulus.

In most of the previous studies, zero strain lengths were derived from anthropomorphic data, not from subject specific data. The one exception is Weimer 2007, in which subject specific zero strain lengths were calculated, although, these were arbitrarily altered to improve the model's performance. All previous studies used 0.03 for the strain level at which the ligament's force length curve transitions from nonlinear to linear, which was experimentally determined by Butler et al. 1986. The proposed idea to do a DOE study on the various ligament properties to come up with subject specific ligament properties is considered novel. The

stiffness parameters of the various ligaments will be included in the study, in order to provide validation of the results.

## CHAPTER 3

### MATERIALS AND METHODS

#### Introduction

Computational models of anatomical based knee joints are useful for investigating the role of different parameters during dynamic motion. It is impossible to directly measure some parameters in vivo without altering the subject physically, thereby altering the subjects natural motion. In the current study, a three-dimensional computational model of a subject-specific human knee in a dynamic simulator was developed based on the work of Weimer 2007. The kinematic results from an experimental and simulated walk cycle were compared for model validation. The validated model was used to study ligament parameters within the knee. The model includes subject-specific geometries of the femur, tibia and patella, and representations of the anterior cruciate ligament (ACL), posterior cruciate ligament (PCL), medial collateral ligament (MCL) and lateral collateral ligament (LCL). The patellar tendon is also represented with three bundles, while the quadriceps tendons are split into four bundles (vastus lateralis (VL), vastus intermedius (VI), vastus medialis (VM) and rectus femoris (RF)). Design of Experiments techniques were used to predict the various parameters in the ligaments used to represent the force-length relationship.

#### Experimental Knee Testing in the Kansas Knee Simulator (KKS)

##### The Knee Specimen

The specimen tested was a human left knee from a 68 year old male donor received on August 24<sup>th</sup>, 2006, designated KN05. The specimen's weight at death was 195 lbs. The knee



was frozen at -20° Celsius from the time it was received. The knee was found to be free of major deformities during visual inspection, and was tested on March 9<sup>th</sup>, 2007.

#### Magnetic Resonance Images (MRI)

MR images of the specimen knee were taken at the Kansas City Imaging Center in Kansas City, Kansas on March 9, 2007. Scans were taken on a 1.5 Tesla Siemens Espree system with a knee coil (Image Size: 512 X 512, Pixel size: 0.35156 X 0.35156 mm). Scans were taken in the sagittal, coronal and axial planes.

#### Dynamic Knee Testing in KKS

The knee specimen was tested in the Kansas Knee Simulator (KKS) located at the University of Kansas Experimental Joint Biomechanics Research Laboratory (Lawrence, Kansas) on March 9<sup>th</sup>, 2007. The KKS is a servo-hydraulic testing machine that can apply dynamic loading to a knee joint. Loads are generated using five hydraulic actuators coupled with five-axis controllers at the proximal femur, distal tibia, and quadriceps tendon (Weimer 2007).

The KKS applies a vertical load at the hip to simulate the body weight of the subject, otherwise, the hip is free to flex extend and translate vertically. Vertical torque, medial-lateral force, and ankle flexion torque loads can be applied at the base of the tibia, and the tibia is free to rotate in varus-valgus motion. The last actuator is attached to the quadriceps tendon proximal to the patella to create a quadriceps load. Each of the axes can be controlled in position or load control. Generally the simulated quadriceps muscle is used to control the flexion angle of the femur at the hip. The other four actuators operate in load control mode to apply dynamic loading at the hip and ankle.

Following the MRI and prior to testing, a parapatellar vastus quad sparing incision was preformed, and a DVRT was placed on the ACL. The fat pad was removed, and a small

notchplasty was performed to protect the DVRT. The femur and tibia were cut and potted into custom fixtures using PolyMethyl MethAcrylat (PMMA). The subject knee was aligned in the KKS by running a walk cycle and adjusting the potting fixtures until the ankle sled showed minimal medial-lateral movement, then tightening the potting fixture set screws.

KN05 was run through a number of different profiles, including laxity, squat and walk cycles. After testing was complete on the natural knee, the ACL was transected, and the knee was again run through many of the profiles, followed by cutting the PCL and again repeating the profiles.

### Point Clouds

Points were taken of the knee aligned in the KKS using a 3-camera Optotrak 3020 system to digitize the points. This was done to ensure modeled knee geometries can be aligned accurately to reflect experimental testing. Points were also taken on the KKS itself, in both the tibia and femur reference frames, to establish a starting position for aligning the machine.

Rigid body kinematics markers, based on the infrared emitting diodes attached to the femur, tibia and patella, in the computational model were used to align the model to the experimental setup. After proper alignment, the markers were used to track the position of the patella and tibia in the femoral coordinate system. The position of each rigid body was represented in the Cartesian X, Y and Z in millimeters and the orientation in the Euler 1-2-3 angles in degrees.

After the completion of experimental testing, the knee was disarticulated and the Optotrak 3020 system was used to digitize point clouds of anatomical features. Point clouds were taken of the insertion and origin sights for the ACL, PCL, MCL, and LCL as well as the articular surfaces of the femur, tibia, and patella.

## Knee Model Construction

### MRI Conversion to 3D Geometries

The software 3D Slicer version 3.4 ([www.slicer.org](http://www.slicer.org)) was used to convert MR images into 3D geometries. Three-dimensional geometries were created for the femur, tibia, fibula and patella. The sagittal view of the MRI was used for manual segmentation. The outer geometry of the desired tissue was traced by hand using a WACOM Cintiq 12WX pen display. A closed polygon was defined for each MRI slice. After all the slices for each geometry were traced, stacking of the slices was accomplished using a marching cubes method, with smoothing of 20 and decimation of 1.

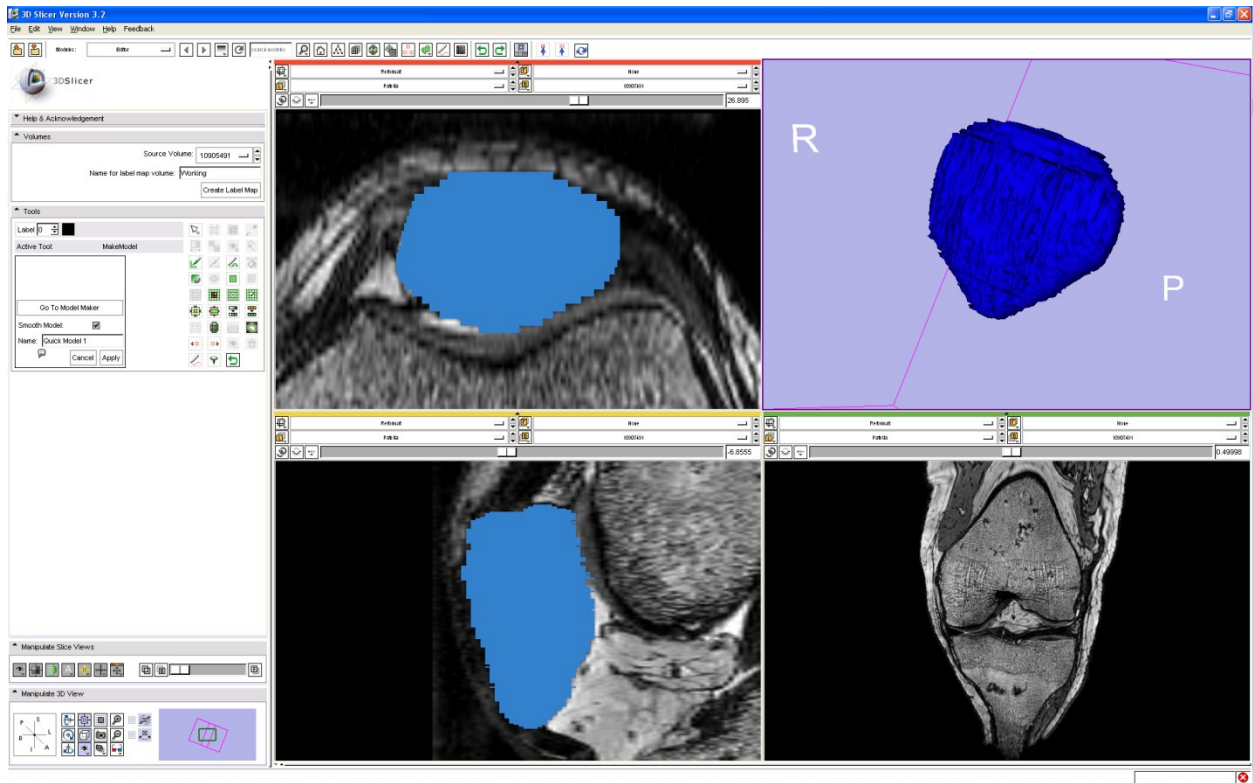


**Figure 1: MRI Tracing and Model Creation Using Slicer 3.4**

## Geomagic

The stereolithography files compiled in Slicer went through a final manipulation in Geomagic Studio 9 (Geomagic, Inc., Triangle Park, North Carolina). The geometries were decimated to reduce file size and computational times. The geometries underwent the following processes in Geomagic:

### Femur with Cartilage:

- Fill Holes
- Remove Spikes: High level
- Reduce Noise: 1 iteration, 1 mm deviation limit
- Decimate:
  - Articular Surface: 6.25%
  - Non Articular Surface: 3.75%

### Tibia with Cartilage:

- Fill Holes
- Remove Spikes: High level
- Reduce Noise: 5 iteration, 1 mm deviation limit
- Decimate:
  - Articular Surface: 6.25%
  - Non Articular Surface: 3.75%

### Fibula:

- Remove Spikes: High level
- Reduce Noise: 5 iteration, 1 mm deviation limit
- Decimate:

- All Surfaces: 3.75%

Patella with Cartilage:

- Remove Spikes: High level
- Reduce Noise: 3 iteration, 1 mm deviation limit
- Decimate:
  - All Surfaces: 6.25%

### Geometry Alignment in Model

Point clouds taken on the KKS machine were imported into MSC.Adams (MSC.Software Corp., Santa Ana, CA). The points were used to visually align the machine and the origin positions of the femur and tibia rigid body kinematic markers relative to the machine. Spheres were created to locate the reference frames for the femur, tibia and patella, and were made part of the respective rigid body to track motions and rotations.



**Figure 2: KKS Alignment Points**



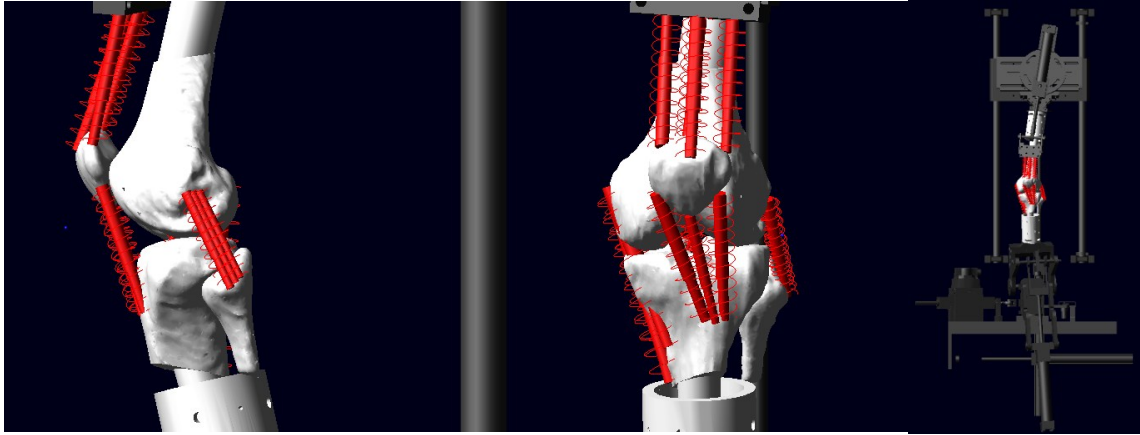


**Figure 4: KN05 Aligned in KKS**

### Ligament and Tendon Representation

Non-linear spring damper elements were used to model ligaments and tendons. The insertion and origin locations were chosen by combining subject specific experimental point clouds, and published data. Three bundles were chosen for the LCL and MCL (Park et al. 2006) and two bundles were chosen for the ACL and PCL (DeFrate et al. 2008, Chhabra et al.2006). The bundles were located visually within the experimental point clouds for each ligament.

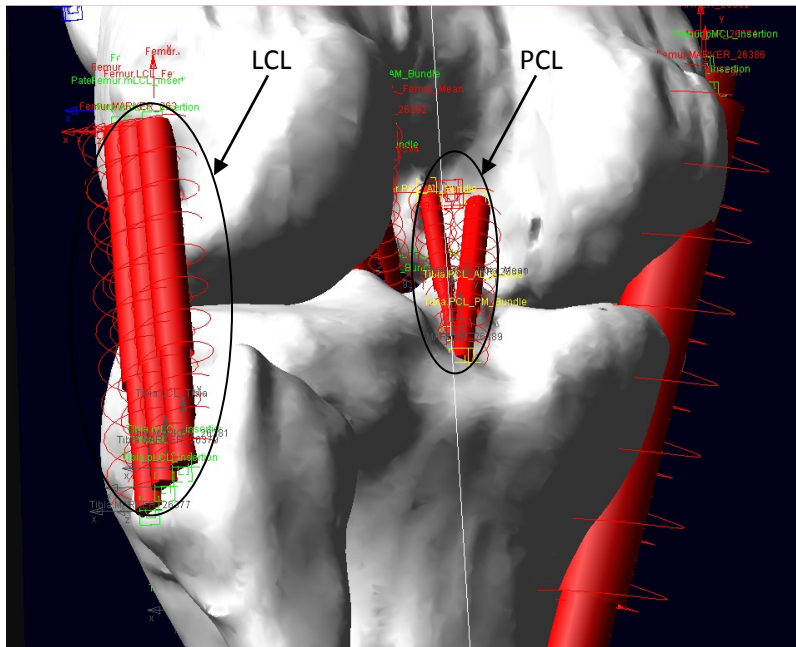


**Figure 5: Ligaments in Model (LCL and PCL)**

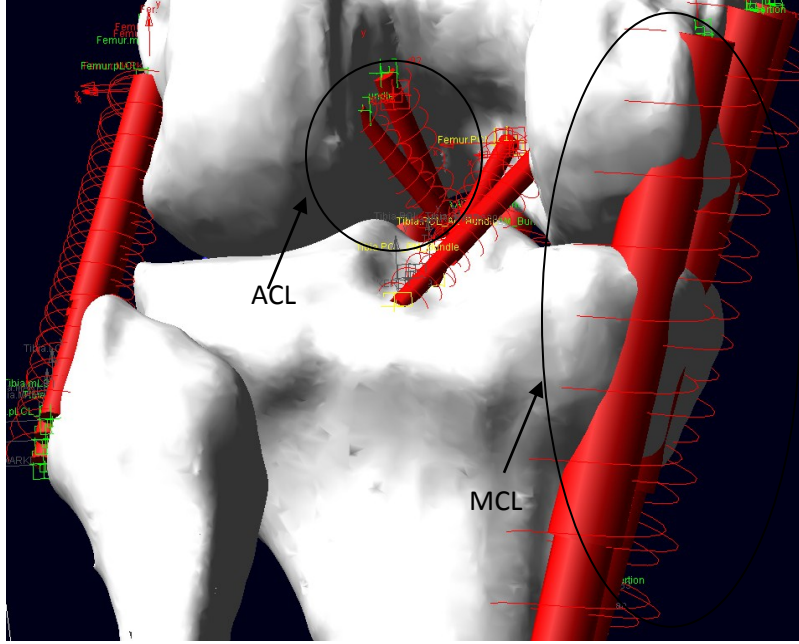


**Figure 6: Ligaments in Model (ACL and MCL)**

The force-displacement curve of each ligament bundle was represented by non-linear splines. The non-linear behavior of the ligaments is described by equations 1 and 2 (Blankevoort et al. 1991):

$$f = \begin{cases} \frac{1}{4} k \varepsilon^2 / \varepsilon_l, & 0 \leq \varepsilon \leq 2\varepsilon_l \\ k(\varepsilon - \varepsilon_l) & \varepsilon > 2\varepsilon_l \\ 0 & \varepsilon < 0 \end{cases} \quad (1)$$

Where  $f$  is the tensile force of the ligament,  $k$  is the ligament stiffness,  $\varepsilon$  is the strain in the ligament, and  $2\varepsilon_l$  is the level at which the ligament moves from the non-linear “toe” region to the linear region of the force-displacement curve. The strain  $\varepsilon$  is described by:

$$\varepsilon = (L - L_0) / L_0 \quad (2)$$

Calculated from the Length  $L$  and the zero strain length  $L_0$  of the ligament.



In order to determine  $L_0$ ,  $k$  and  $\varepsilon_l$  for a subject specific model, a three-level full factorial design was done, optimizing the three factors based on root mean squared (rms) error of the TFJ, the PFJ and the quadriceps force during a walk cycle.

### Experimental Zero Strain Length

During experimental testing the envelope of motion for the subject knee was recorded using the motion capture system. The knee was moved through its envelope of motion, while as little force was exerted on the knee as possible. The resulting envelope profiles were then used to determine experimental zero strain length for each ligament in the knee.

A MatLab m-file was used to determine the experimental zero strain length. The ligament point clouds can be inserted into Lig\_lenth\_crunch.m (appendix), and a center point for the ligament will be created. However, specific insertion sites can be selected, and used as inputs to the m-file, if desired. This allows for more complex ligament representations, such as multiple bundles per ligament. The m-file determines the maximum distance between the insertion point and origin point for each ligament/ligament bundle. These values are then inserted into the spline creation spreadsheet as  $L_0$ .

### Spline Creation Spreadsheet

Slack Length	Double Bundle ACL									
100%	aACL					pACL				
		Ke	5000	5000			Ke	5000	5000	
K Percentage		EI	0.03	0.03			EI	0.03	0.03	
100%		Lsl	4.0300806				Lsl	3.6918713		
		Lm	36.505313				Lm	29.131078		
EI Percentage		Lo	40.535393				Lo	32.82295		
100%										
	I	E	Force	*	Force	I	E	Force	*	Force
	6.86	-0.831	28765.122	-29.65	0.000	-0.52	-1.016	42994.558	-29.65	0.000
	6.91	-0.830	28679.779	-29.60	0.000	-0.47	-1.014	42865.704	-29.60	0.000
	6.96	-0.828	28594.562	-29.55	0.000	-0.42	-1.013	42737.043	-29.55	0.000
	7.01	-0.827	28509.472	-29.50	0.000	-0.37	-1.011	42608.576	-29.50	0.000
	7.06	-0.826	28424.509	-29.45	0.000	-0.32	-1.010	42480.302	-29.45	0.000
	7.11	-0.825	28339.673	-29.40	0.000	-0.27	-1.008	42352.222	-29.40	0.000
	7.16	-0.823	28254.963	-29.35	0.000	-0.22	-1.007	42224.335	-29.35	0.000
	7.21	-0.822	28170.380	-29.30	0.000	-0.17	-1.005	42096.641	-29.30	0.000

**Figure 7: Example of Spline Creation Spreadsheet**

Microsoft Excel was used to create the ligament force-displacement splines. Various parameters were needed in order to create the force-displacement splines.  $K_e$  in the spreadsheet is the ligament stiffness parameter, with the initial value being taken from Blankevoort et al. 1991, then being manipulated by multiplying by the “K Percentage” parameter. The initial stiffness parameters were:

**Table 1: Ligament Stiffness Parameters (Blankevoort et al., 1991)**

Ligament	Ligament Bundle	k [N]
Anterior Cruciate Ligament	aACL	5000
	pACL	5000
Posterior Cruciate Ligament	aPCL	9000
	pPCL	9000
Lateral Collateral Ligament	aLCL	2000
	sLCL	2000
	pLCL	2000
Medial Collateral Ligament	aMCL	2750
	iMCL	2750
	pMCL	2750

$E_l$  is  $\varepsilon_l$ , which is used to determine where the force-displacement curve changes from the non-linear “toe” region to the linear portion.  $L_m$  is the measured length of the ligaments from MSC.Adams with the KKS in its alignment position, whereas  $L_o$  is the experimentally determined ligament zero strain length.  $L_{sl}$  is the difference between  $L_o$  and  $L_m$ . If  $L_{sl}$  is positive, the ligament is slack, and if it is negative, the ligament is in tension.  $E$  is calculated using equation 2, and then the force is calculated using equation 1. The column ‘\*’ is used as the displacement of the ligament with respect to  $L_m$ . The second force column uses an ‘IF’

statement to determine which part of the piecewise equation to use and to calculate the force due to the displacement (figure 3).

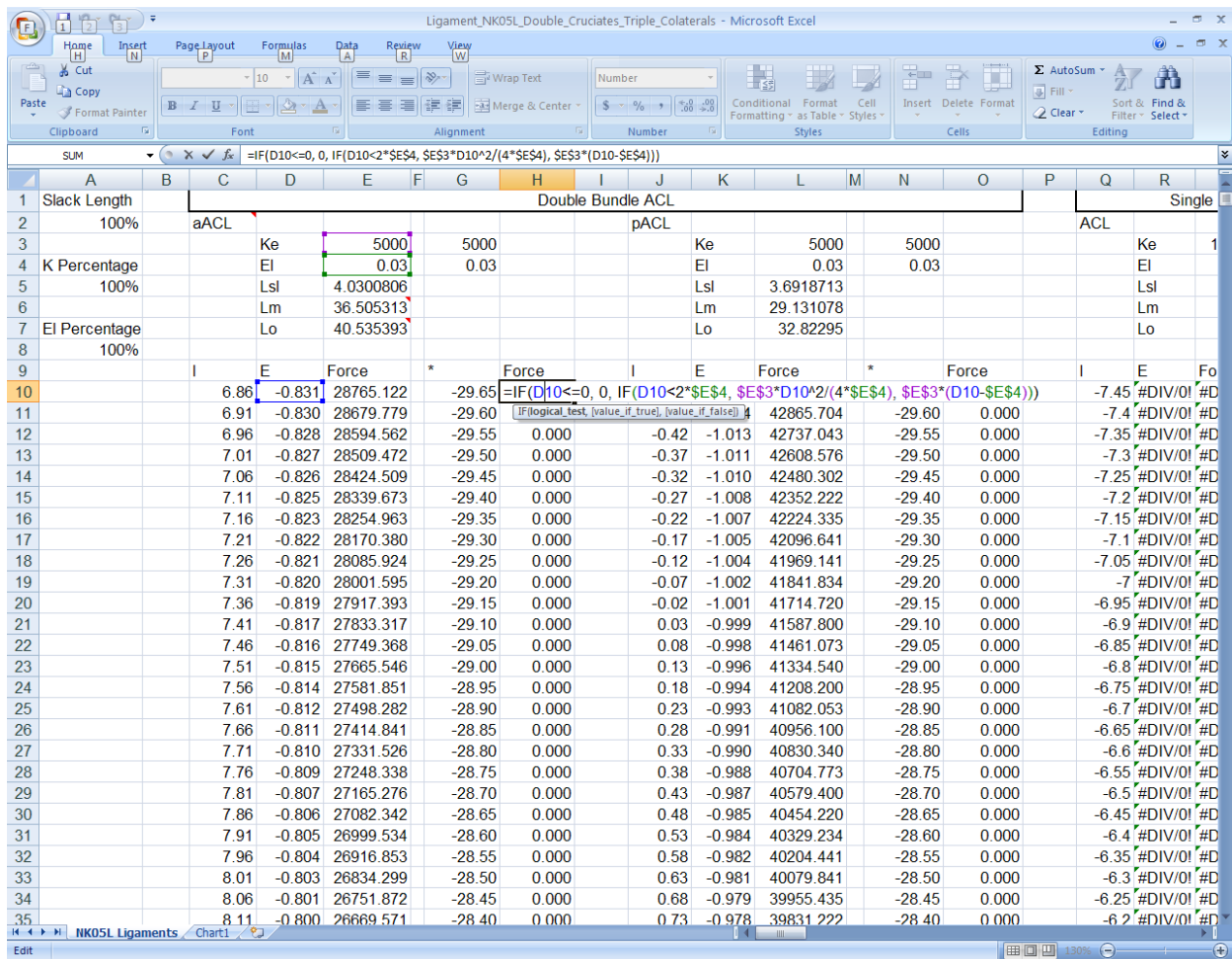


**Figure 8: Spline Creation Spreadsheet with Piecewise Equation Shown**

The last two columns are copied into MSC.Adams to create the splines. These splines are then selected for use in the appropriate ligament springs.

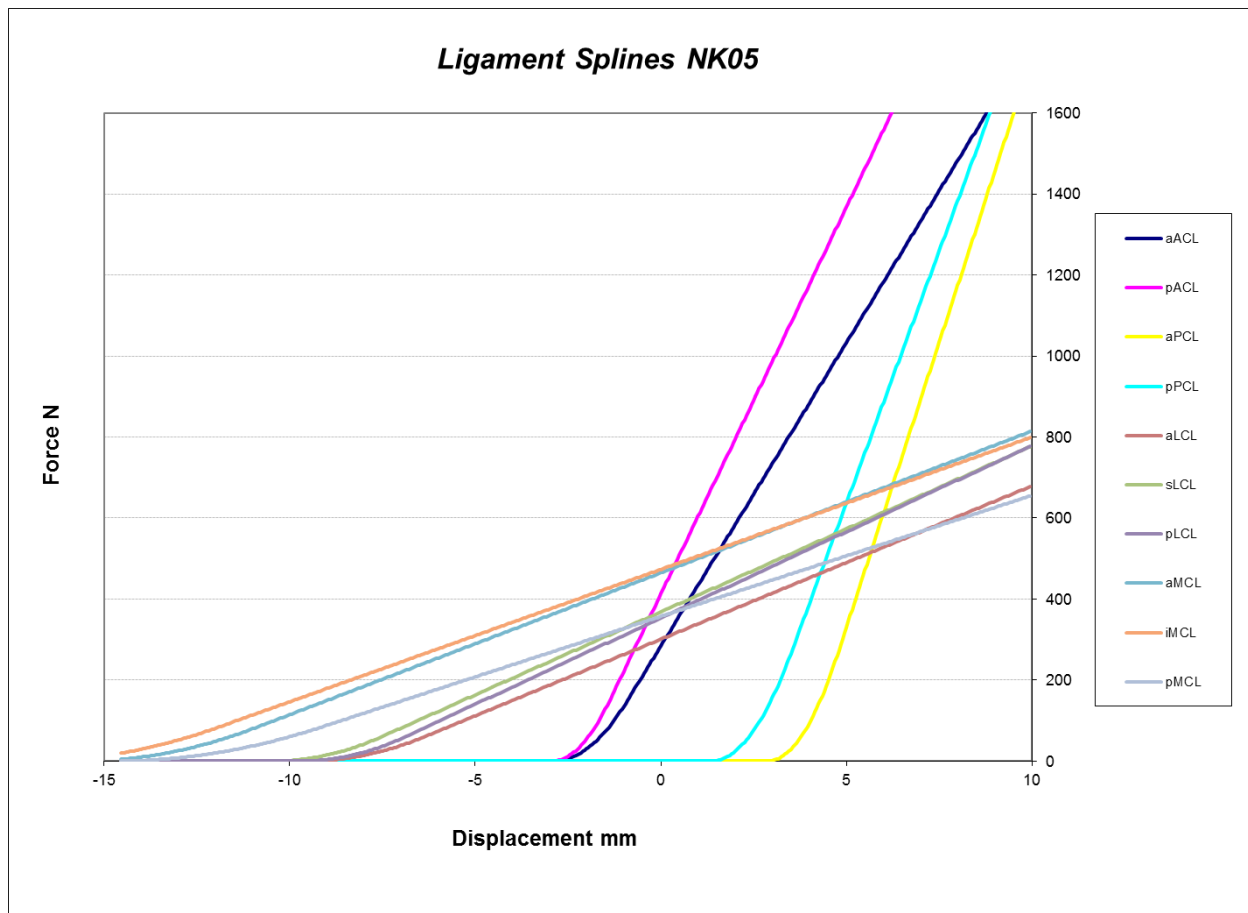


**Figure 9: Ligament Force Splines Based on 80% of Experimental Zero Strain Length**

### Knee Model Simulation

#### Simulation Profile

During experimental testing, several profiles were run in the KKS simulator. A ten second walk profile was selected for ligament optimization. Two cycles of the profile were simulated.

In the computational multibody KKS model developed in MSC.Adams, the input forces are applied through a PID control. The control plant takes data from MSC.Adams, sends it through the PID controls, and sends the output back to MSC.Adams to compute the next step. Parameters from Weimer 2007 were used to come up with PID parameters for use in the current model.

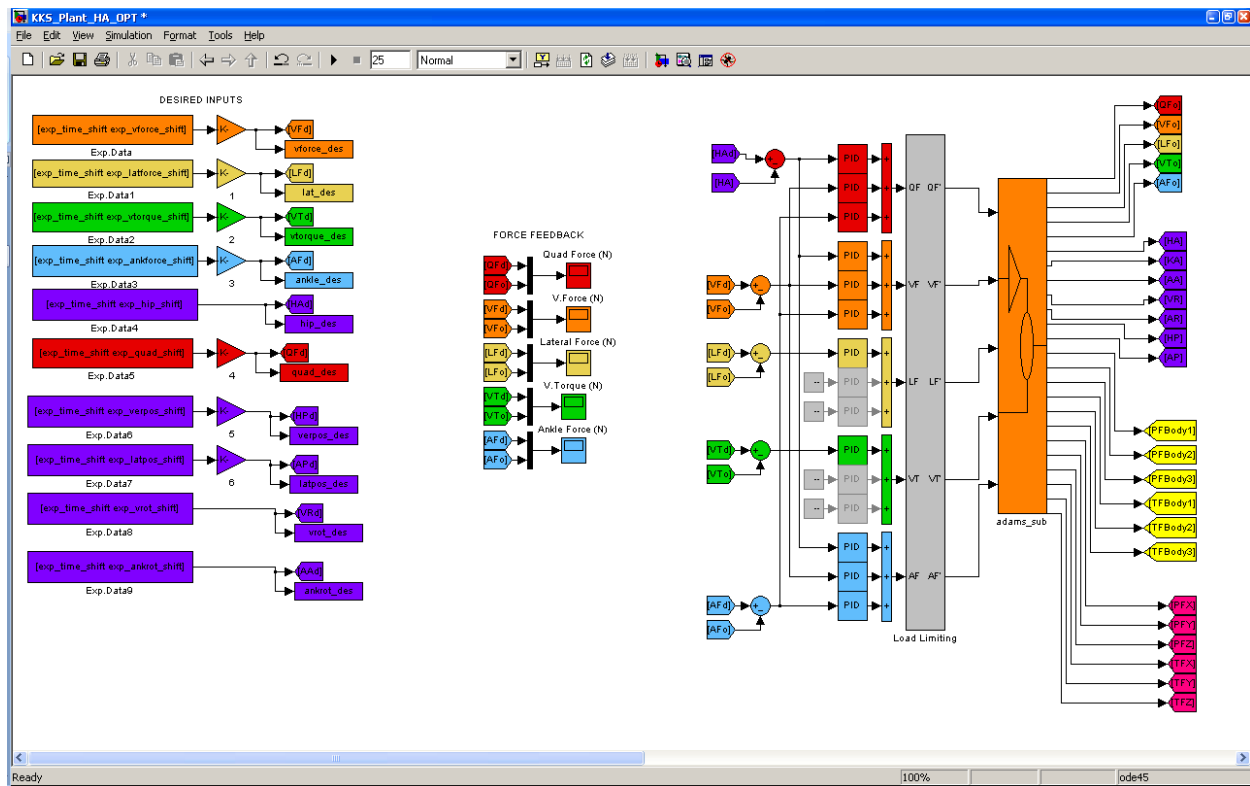
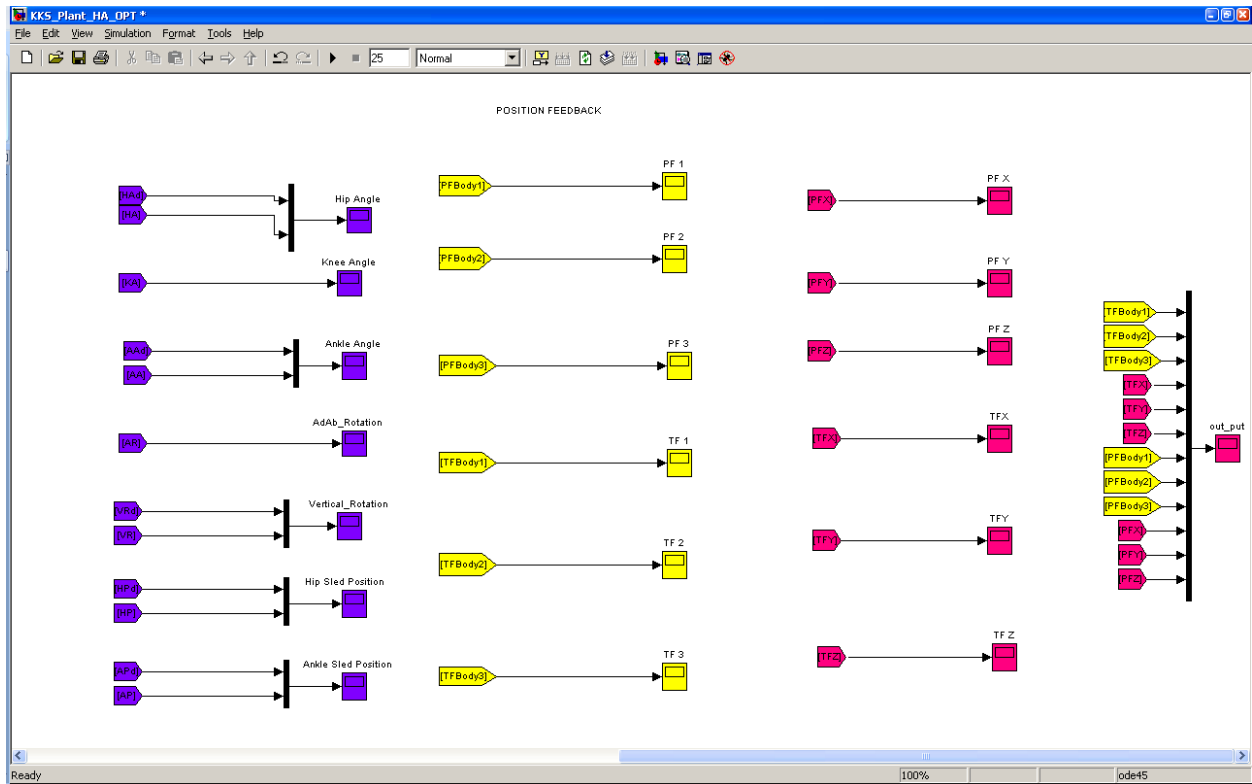


Figure 10: Simulink Control Plant with PID Parameters



**Figure 11: Simulink Control Plant Position Feedback**

After a simulation, it is necessary to remove any phase shift between the experimental data relative to the simulation data. This is accomplished in MatLab, comparing the experimental results and the simulation results of the most dynamically active coordinate. The MatLab script shifts the chosen coordinate's simulation results, and computes the RMS error between the simulation and the experimental results, until it finds a minimum. The time shifted results are then used to calculate final RMS errors, which will be used for optimization using DOE methods.

### Design of Experiments (DOE)

Design of Experiments (DOE) deals with systematically changing a set of inputs in order to observe the corresponding changes to the output. The objective is to use statistical methods to

determine which variables are most important to the output response and to assign values to those variables. Two different DOE methods were used in the current study.

*Two level partial factorial design:*

First a two-level fractional factorial design was employed to determine if the system responded linearly to the changes in the inputs and each input's significance. As mentioned earlier, the inputs used were:  $L_0$ ,  $k$  and  $\varepsilon_l$ . The two-level fractional factorial design with the three parameters required running four simulations, changing each parameter to either the low or high value (represented by -1 or 1 respectively). For  $k$  and  $\varepsilon_l$  the low and high values were decided to be 50% (-1) and 150% (1) of the values used in Weimer 2007. For  $L_0$  these values were set at 60% and 100% of the experimentally determined zero load length.

**Table 2: Two-level Fractional Factorial Design Parameters**

Run	A	B	C	D	E	F	Y
1	a <sub>1</sub>	b <sub>1</sub>	c <sub>1</sub>	d <sub>1</sub>	e <sub>1</sub>	f <sub>1</sub>	Y <sub>1</sub>
2	a <sub>2</sub>	b <sub>2</sub>	c <sub>2</sub>	d <sub>2</sub>	e <sub>2</sub>	f <sub>2</sub>	Y <sub>2</sub>
3	a <sub>3</sub>	b <sub>3</sub>	c <sub>3</sub>	d <sub>3</sub>	e <sub>3</sub>	f <sub>3</sub>	Y <sub>3</sub>
4	a <sub>4</sub>	b <sub>4</sub>	c <sub>4</sub>	d <sub>4</sub>	e <sub>4</sub>	f <sub>4</sub>	Y <sub>4</sub>

The A and B parameters are set to either 1 or -1, and the C parameter condition is determined by  $C = A * B$  for a fractional factorial design. This keeps the number of distinct runs to 4, thus decreasing computational time.

The effect of each parameter is determined using equations 3:

$$\Delta_m = m = \frac{\sum_{i=1}^n m_i Y_i}{2} \quad (3)$$

where m is : a, b, c, etc.

The effect of a parameter gives an indication of how that parameter affects the output response. If the effect is zero, this indicates that parameter has no effect on the output. A positive effect suggests that increasing the parameter will increase the output and a negative effect suggests the opposite.

The contribution of each factor is calculated according to equations 4 and 5.

$$\text{Contribution} : \frac{\Delta_m^2}{T} 100\% \quad (4)$$

$$T = \sum_{i=1}^n m_i^2 \quad (5)$$

The contribution of a factor is a way to quantify the effect of a parameter into a percentage, for easy comparison. If a factor's contribution is under a preset value (5% for example), then that factor can be eliminated from the prediction equations, because it has an insignificant affect on the output response.

The outcome can then be predicted based on equations 6 and 7, which assumes the output responds linearly to the input. The linearity of the system can then be checked by running a simulation at the median values of each parameter, and checking the results versus the predicted response.

$$\hat{Y}_i = \bar{Y} + \frac{a}{2} A + \frac{b}{2} B + \frac{c}{2} C + \frac{d}{2} D + \frac{e}{2} E + \frac{f}{2} F \quad (6)$$

$$\bar{Y} = \frac{\sum_{i=1}^n Y_i}{n} \quad (7)$$

As mentioned before, any of the  $\frac{m}{2} M$  terms can be removed, if the respective parameter does not show a high enough contribution.



In order to evaluate the predictive power of the prediction equation, an ANOVA calculation is done. Using equations 8 – 11, the adjusted coefficient of determination,  $R_a^2$ , can be calculated. If this value is less than 0.8, this suggests that the prediction equation adequately fits the data.

$$e_i = Y_i - \hat{Y}_i \quad (8)$$

$$SST = \sum_{i=1}^n Y_i^2 - n\bar{Y}^2 \quad (9)$$

$$SSE = \sum_{i=1}^n e_i^2 \quad (10)$$

$$R_a^2 = 1 - \left( \frac{n-1}{n-p} \right) \frac{SSE}{SST} \quad (11)$$

The error between the prediction equation result and the experimental result is represented by  $e_i$ . The SST is the corrected total sum of squares, and the SSE is the error sum of squares. The value n represents the number of experimental runs, and p represents the number of terms in the prediction equation.

If the prediction equation developed during the two level fractional factorial design does not adequately predict the output, then a more sophisticated method is required. The next method used is dependent on why the first method did not fit well.

*Three level full factorial design:*

A three level design requires testing of a third level for each parameter. This increases the number of distinct simulations significantly. Running a three level design is required if the two level design shows that the prediction equation is nonlinear.

A full factorial design requires that factor C is determined independently of factors A and B, as opposed to computing factor C as  $C = A * B$  for the partial factorial design. A full factorial

design is required if factor C is shown to be significant to the prediction equation. This also increases the number of distinct simulations significantly.

If the system is shown to be nonlinear and factor C is shown to be significant to the prediction equation, then a Three Level Full Factorial Design is required to accurately predict the systems response.

A Three Level Full Factorial Design uses a general linear model to predict the response of the system. Equation 12 shows the general linear model.

$$\bar{Y} = \bar{X} \bar{\beta} + \bar{\epsilon} \quad (12)$$

Where  $\bar{Y}$ ,  $\bar{X}$ ,  $\bar{\beta}$ , and  $\bar{\epsilon}$  are:

$$\bar{Y} = \begin{bmatrix} Y_1 \\ . \\ . \\ . \\ . \\ Y_{27} \end{bmatrix} \quad (13)$$

$$\bar{X} = \begin{bmatrix} 1 & x_{11} & x_{21} & x_{31} & x_{11}x_{21} & x_{11}x_{31} & x_{21}x_{31} & x_{11}^2 & x_{21}^2 & x_{31}^2 \\ . & . & . & . & . & . & . & . & . & . \\ . & . & . & . & . & . & . & . & . & . \\ . & . & . & . & . & . & . & . & . & . \\ 1 & x_{127} & x_{227} & x_{327} & x_{127}x_{227} & x_{127}x_{327} & x_{227}x_{327} & x_{127}^2 & x_{227}^2 & x_{327}^2 \end{bmatrix} \quad (14)$$

$$\bar{\beta} = \begin{bmatrix} \beta_0 \\ \beta_1 \\ \beta_2 \\ \beta_3 \\ \beta_{12} \\ \beta_{13} \\ \beta_{23} \\ \beta_{11} \\ \beta_{22} \\ \beta_{33} \end{bmatrix} \quad (15)$$

$$\epsilon = \begin{bmatrix} \epsilon_1 \\ \cdot \\ \cdot \\ \cdot \\ \cdot \\ \epsilon_{27} \end{bmatrix} \quad (16)$$

$\bar{Y}$  is the true response of the system.  $\bar{X}$  is the systems inputs, determined, as in the partial factorial design, to be a percentage of the parameters  $L_0$ ,  $k$  and  $\varepsilon_l$ . The factor  $\bar{\beta}$  is a vector parameter of regression coefficients, and  $\epsilon$  is a vector of random errors (Rekab and Shaikh 193).

In order to estimate the system response, the estimated regression equation must be used (equation 17). This allows for the estimated regression coefficients,  $\bar{b}$ , to be calculated using equation 19. Equation 19 is determined with the objective of minimizing  $e'e$ , where  $e$  is represented by equation 20.

$$\hat{Y} = \bar{X} \bar{b} \quad (17)$$

$$\bar{b} = \begin{bmatrix} b_0 \\ b_1 \\ b_2 \\ b_3 \\ b_{12} \\ b_{13} \\ b_{23} \\ b_{11} \\ b_{22} \\ b_{33} \end{bmatrix} \quad (18)$$

$$\bar{b} = (\bar{X}' \bar{X})^{-1} \bar{X}' \bar{Y} \quad (19)$$

$$e = \bar{Y} - \hat{Y} \quad (20)$$

*Significance of regression parameters:*

The estimated regression equation allows for the prediction of the outcome of the system to be based only on the intended input. Before optimization of the regression equation, it is necessary to determine which factor's effects are important to the outcome of the prediction equation. In order to evaluate each factor's significance, a student t test can be done.

$$T_0 = \frac{b_k}{S(b_k)} \quad (21)$$

Where  $b_k$  is the  $k^{\text{th}}$  regression coefficient from equation 18, and  $S^2(b_k)$  is the  $k^{\text{th}}$  diagonal element of the estimated variance-covariance matrix  $S^2(b)$ .

$$S^2(b) = MSE(\bar{X}' \bar{X})^{-1} \quad (22)$$

$$MSE = \frac{\sum_{i=1}^n e_i^2}{n - L - 1} \quad (23)$$

Next,  $T^*$  is acquired from t distribution table, such as the one in Appendix 5 in *Statistical Design of Experiments with Engineering Applications* (Rekab and Shaikh).

$$T^* = t(\alpha/2, n-L-1) \quad (24)$$

Equation 24 has  $n-L-1$  degrees of freedom.  $n$  is the number of observations and  $L$  is the number of terms, excluding  $\beta_0$ . Equation 25 is used to calculate  $\alpha$  after a desired % confidence is selected.

$$\alpha = [100 - (\% \text{ Confidence})]/100. \quad (25)$$

If  $|T_0| > T^*$  then the term is significant to the prediction equation. However, if  $|T_0| < T^*$ , then the term is not significant to the prediction equation and should be excluded.

The final regression equation is represented by equation 26.

$$\hat{Y} = b_0 + b_1x_1 + b_2x_2 + b_3x_3 + b_{12}x_1x_2 + b_{13}x_1x_3 + b_{23}x_2x_3 + b_{11}x_1^2 + b_{22}x_2^2 + b_{33}x_3^2 \quad (26)$$

Any term that was determined to be insignificant to the regression model should be excluded from the final regression equation. This is done by setting the estimated regression coefficient,  $b_k$ , to zero. For example, if the term  $x_1$  is insignificant, then  $b_1 = 0$ .

*Optimization of the regression equation:*

The regression equation (Equation 26) can be rearranged as follows:

$$\hat{Y} = b_0 + \bar{X}'\bar{b} + \bar{X}'\bar{B}\bar{X} \quad (27)$$

Where:

$$\bar{X} = \begin{bmatrix} x_1 \\ x_2 \\ x_3 \end{bmatrix} \quad (28)$$

$$\bar{b} = \begin{bmatrix} b_1 \\ b_2 \\ b_3 \end{bmatrix} \quad (29)$$

$$\bar{B} = \begin{bmatrix} b_{11} & b_{12}/2 & b_{13}/2 \\ b_{12}/2 & b_{22} & b_{23}/2 \\ b_{13}/2 & b_{23}/2 & b_{33} \end{bmatrix} \quad (30)$$

The stationary, or critical point, is the point at which the first derivative of  $\hat{Y}$  with respect to  $\bar{X}$  is zero. Matrix differentiation of Equation 27 yields:

$$\frac{d\hat{Y}}{d\bar{X}} = \bar{b} + 2\bar{B}\bar{X} \quad (31)$$

The stationary point is represented by  $\bar{X}_0$ .

$$\bar{X}_0 = -\frac{1}{2}\bar{B}'\bar{b} \quad (32)$$

The stationary point represents the optimal conditions for the system. The optimal  $\hat{Y}_0$  is calculated by substituting  $\bar{X}_0$  into equation 27.

In order to optimize the regression equation, the results of the simulations needed to be normalized, since translational RMS errors are in millimeters, rotational RMS errors are in degrees and machine RMS errors are in newtons. This was accomplished by dividing by the highest RMS error in each category, making the highest RMS error one, and all others a decimal between zero and one. By normalizing each category of RMS error, the units were removed, and comparisons between categories became relevant. The RMS error categories were then grouped into femur, patella or machine groups, and different weights were assigned to each group in order to evaluate optimization based on different groups of results. The femur and patella groups each have six categories (X, Y, Z, rotation 1, rotation 2, and rotation 3), but the machine group

only has one parameter. In order to evaluate each group with equal weighting, the machine group is multiplied by six.

## CHAPTER 4

### RESULTS

A ten second walk profile was selected for ligament optimization, and two cycles of the profile were simulated. RMS error from the selected profile will be used for optimization using DOE methods.

#### Two Level Partial Factorial Design

First a two level partial factorial design was completed, using the ligament zero load lengths ( $L_0$ ) and stiffness ( $k$ ) as the main factors and  $\varepsilon_l$  as the dependant factor. The experiment required five simulations, as shown in Table 3. Each simulation was run in MSC.Adams, and RMS errors were calculated using Matlab.

**Table 3: Two Level Partial Factorial Design**

Run	A ( $L_0$ )	B ( $k$ )	C ( $\varepsilon_l$ )	D (AB)	E (AC)	F (BC)	G (ABC)
1	1	1	1	1	1	1	1
2	-1	1	-1	-1	1	-1	1
3	1	-1	-1	-1	-1	1	1
4	-1	-1	1	1	-1	-1	1
0	0	0	0	0	0	0	0

Factors A, B and C represent the individual effects of each parameter, while factors D through G represent the effects of the interactions between the parameters.

For each run, Body 1, 2, 3 and Cartesian X, Y, Z RMS errors were calculated for both the tibia and the patella based on the femoral coordinate system. The rigid body marker on the femur is aligned such that the Cartesian X coordinate is primarily aligned with the medial-lateral directions of the femur, the Cartesian Y coordinate is primarily aligned with the anterior-posterior directions of the femur, and the Cartesian Z coordinate is primarily aligned along the



shaft of the femur. On the tibia the rigid body marker is aligned such that the Cartesian X coordinate is primarily aligned with the medial-lateral directions of the tibia, the Cartesian Y coordinate is primarily aligned with the anterior-posterior directions of the tibia, and the Cartesian Z coordinate is primarily aligned along the shaft of the tibia. The patella rigid body marker is aligned such that the Cartesian X coordinate is primarily aligned with the anterior-posterior directions of the patella, the Cartesian Y coordinate is primarily aligned with the proximal-distal directions of the leg, and the Cartesian Z coordinate is primarily aligned with the medial-lateral directions of the patella. The Body 1, 2, and 3 rotations refer to the orientation of the tibia and patella with respect to the femur in order of X, Y, and Z. The RMS errors were used to develop prediction equations and verify the accuracy of the regression equation. The sum of errors (SUM) was used to calculate the average error, and the average of errors (AVE) was used to calculate the total sum of squares (SST).

**Table 4: Tibia RMS Errors**

Tibia						
Run	Body1	Body2	Body 3	X	Y	Z
1	5.00	4.45	28.65	46.80	9.43	9.47
2	2.27	2.14	12.86	7.67	4.79	5.79
3	41.00	12.53	6.22	54.30	43.64	109.71
4	2.24	2.09	12.82	8.47	4.32	6.24
0	2.49	1.77	14.10	7.96	3.14	8.46
SUM	50.51	21.21	60.56	117.24	62.18	131.22
AVE	12.63	5.30	15.14	29.31	15.55	32.81

**Table 5: Patella RMS Errors**

Patella						
Run	Body1	Body2	Body 3	X	Y	Z
1	6.10	4.24	17.22	4.37	6.78	10.47
2	3.26	3.11	17.85	5.27	6.35	16.40
3	45.70	65.03	84.40	41.24	66.28	72.21
4	4.31	3.46	18.56	4.66	4.30	13.35
0	5.27	3.68	18.80	4.70	3.89	11.53
SUM	59.36	75.85	138.04	55.54	83.71	112.43
AVE	14.84	18.96	34.51	13.88	20.93	28.11

The effect of each factor is then calculated based on the output response of the system.

This has to be done separately for all 12 outputs. If the effect is greater than 5%, then the factor is significant to the prediction equation.

**Table 6: Effects Calculated from the Tibia Coordinate System**

Tibia								
K Number of distinct runs	4							
m Number of factors	7							
	a	b	c	d	e	f	g	T
Main effect on Body 1	20.74	-17.99	-18.01	-18.01	-17.99	20.74	25.26	2794.49
	15%	12%	12%	12%	12%	15%	23%	
Main effect on Body 2	6.38	-4.02	-4.07	-4.07	-4.02	6.38	10.60	259.14
	16%	6%	6%	6%	6%	16%	43%	
Main effect on Body 3	4.59	11.23	11.20	11.20	11.23	4.59	30.28	1462.24
	1%	9%	9%	9%	9%	1%	63%	
Main effect on X	42.48	-4.15	-3.35	-3.35	-4.15	42.48	58.62	7103.17
	25%	0%	0%	0%	0%	25%	48%	
Main effect on Y	21.98	-16.87	-17.34	-17.34	-16.87	21.98	31.09	3103.24
	16%	9%	10%	10%	9%	16%	31%	
Main effect on Z	53.58	-50.35	-49.89	-49.89	-50.35	53.58	65.61	20093.92
	14%	13%	12%	12%	13%	14%	21%	

**Table 7: Effects Calculated from the Patella Coordinate System**

Patella								
K Number of distinct runs	4							
m Number of factors	3							
	a	b	c	d	e	f	g	T
Main effect on Body 1	22.11	-20.33	-19.27	-19.27	-20.33	22.11	29.68	3428.18
	14%	12%	11%	11%	12%	14%	26%	
Main effect on Body 2	31.35	-30.57	-30.22	-30.22	-30.57	31.35	37.93	7099.48
	14%	13%	13%	13%	13%	14%	20%	
Main effect on Body 3	32.60	-33.94	-33.24	-33.24	-33.94	32.60	69.02	11402.92
	9%	10%	10%	10%	10%	9%	42%	
Main effect on X	17.84	-18.14	-18.74	-18.74	-18.14	17.84	27.77	2767.90
	11%	12%	13%	13%	12%	11%	28%	
Main effect on Y	31.21	-28.72	-30.78	-30.78	-28.72	31.21	41.86	7243.93
	13%	11%	13%	13%	11%	13%	24%	
Main effect on Z	26.47	-29.35	-32.39	-32.39	-29.35	26.47	56.21	8381.93
	8%	10%	13%	13%	10%	8%	38%	

The main factors (A, B, and C) are significant for all of the output models, except for the Tibia Body 3 model, where factor A is not significant, and the Tibia X model, where factors B and C are not significant. The interaction factors (D, E, F, and G) are significant for all of the output models except for the Tibia Body 3 model, where effect F is not significant, and the Tibia X model, where effects D and E are not significant. These results indicate that the partial factorial design is not sufficient to represent the model, and that a full factorial design needs to be done to get a full representation of the effect of factor C.

After completion of runs 1 – 4, a prediction equation was developed, and the error between the actual RMS errors and the predicted RMS errors were calculated. Run 0 is used to evaluate the median values of the system, and to verify the results.

**Table 8: Predicted Tibia RMS Errors**

Predicted Tibia						
Run	Body1	Body2	Body 3	X	Y	Z
1	10.00	8.89	57.31	93.61	18.87	18.95
2	4.54	4.28	25.72	15.34	9.58	11.58
3	82.00	25.07	12.44	108.60	87.28	219.43
4	4.49	4.17	25.65	16.93	8.64	12.49
0	12.63	5.30	15.14	29.31	15.55	32.81

**Table 9: Predicted Patella RMS Errors**

Predicted Patella						
Run	Body1	Body2	Body 3	X	Y	Z
1	12.20	8.49	34.45	8.73	13.57	20.94
2	6.51	6.22	35.71	10.54	12.71	32.79
3	91.39	130.07	168.80	82.49	132.56	144.42
4	8.62	6.93	37.12	9.33	8.59	26.70
0	14.84	18.96	34.51	13.88	20.93	28.11

**Table 10: Tibia Prediction Errors**

Error Tibia						
Run	Body1	Body2	Body 3	X	Y	Z
1	-5.00	-4.45	-28.65	-46.80	-9.43	-9.47
2	-2.27	-2.14	-12.86	-7.67	-4.79	-5.79
3	-41.00	-12.53	-6.22	-54.30	-43.64	-109.71
4	-2.24	-2.09	-12.82	-8.47	-4.32	-6.24
0	-10.14	-3.54	-1.04	-21.35	-12.41	-24.34

**Table 11: Patella Prediction Errors**

Error Patella						
Run	Body1	Body2	Body 3	X	Y	Z
1	-6.10	-4.24	-17.22	-4.37	-6.78	-10.47
2	-3.26	-3.11	-17.85	-5.27	-6.35	-16.40
3	-45.70	-65.03	-84.40	-41.24	-66.28	-72.21
4	-4.31	-3.46	-18.56	-4.66	-4.30	-13.35
0	-9.57	-15.28	-15.71	-9.19	-17.04	-16.57

Finally, the coefficient of determination ( $R_a^2$ ) is calculated to verify if the prediction equation fits the model. If  $R_a^2$  is less than 0.8, then the prediction equation adequately fits the model, otherwise, it does not.

**Table 12: Tibia Coefficients of Determination**

Tibia						
	Body 1	Body 2	Body 3	X	Y	Z
d Number of experimental runs	4	4	4	4	4	4
p Number of terms in prediction equation	7	7	7	7	7	7
SSE	1716.20	185.78	1189.54	5269.77	2034.97	12199.34
SST	1078.29	73.36	272.70	1833.39	1068.28	7894.58
Ra Square	4.18	6.06	9.72	6.75	4.81	4.09
Ra Square is greater than 0.8	Yes	Yes	Yes	Yes	Yes	Yes

**Table 13: Patella Coefficients of Determination**

Patella						
	Body 1	Body 2	Body 3	X	Y	Z
d Number of experimental runs	4	4	4	4	4	4
p Number of terms in prediction equation	7	7	7	7	7	7
SSE	2246.06	4502.54	8329.93	1853.92	4788.35	6045.67
SST	1301.45	2844.08	3673.24	1020.45	2761.07	2743.97
Ra Square	4.45	4.17	5.54	4.63	4.47	5.41
Ra Square is greater than 0.8	Yes	Yes	Yes	Yes	Yes	Yes

As shown above in tables 12 and 13, the linear prediction equation does not adequately fit any of the 12 outputs of the model. This shows that a more sophisticated modeling technique is required to fit the model.

### Three Level Full Factorial Design

A three level full factorial design was completed to fully understand the effects of each parameter, and to optimize those parameters for future use in computational knee modeling. The same parameters were used from the two level partial factorial design.  $X_1$  represents  $L_0$ ,  $X_2$  represents  $k$ , and  $X_3$  represents  $\varepsilon_l$ . Unlike the partial factorial design,  $\varepsilon_l$  is not a dependant

factor. Main effects, interactions, and quadratic effects are included in the second order model.

The design matrix  $\bar{X}$  is shown in Table 14.

**Table 14: Design Matrix**

Run	1	X1	X2	X3	X1*X2	X1*X3	X2*X3	X1 <sup>2</sup>	X2 <sup>2</sup>	X3 <sup>2</sup>
1	1	1	1	1	1	1	1	1	1	1
2	1	1	1	0	1	0	0	1	1	0
3	1	1	1	-1	1	-1	-1	1	1	1
4	1	1	0	1	0	1	0	1	0	1
5	1	1	0	0	0	0	0	1	0	0
6	1	1	0	-1	0	-1	0	1	0	1
7	1	1	-0.75	1	-0.75	1	-0.75	1	0.563	1
8	1	1	-0.75	0	-0.75	0	0	1	0.563	0
9	1	1	-0.75	-1	-0.75	-1	0.75	1	0.563	1
10	1	0	1	1	0	0	1	0	1	1
11	1	0	1	0	0	0	0	0	1	0
12	1	0	1	-1	0	0	-1	0	1	1
13	1	0	0	1	0	0	0	0	0	1
14	1	0	0	0	0	0	0	0	0	0
15	1	0	0	-1	0	0	0	0	0	1
16	1	0	-0.75	1	0	0	-0.75	0	0.563	1
17	1	0	-0.75	0	0	0	0	0	0.563	0
18	1	0	-0.75	-1	0	0	0.75	0	0.563	1
19	1	-1	1	1	-1	-1	1	1	1	1
20	1	-1	1	0	-1	0	0	1	1	0
21	1	-1	1	-1	-1	1	-1	1	1	1
22	1	-1	0	1	0	-1	0	1	0	1
23	1	-1	0	0	0	0	0	1	0	0
24	1	-1	0	-1	0	1	0	1	0	1
25	1	-1	-0.75	1	0.75	-1	-0.75	1	0.563	1
26	1	-1	-0.75	0	0.75	0	0	1	0.563	0
27	1	-1	-0.75	-1	0.75	1	0.75	1	0.563	1

Twenty seven simulations were completed, and errors in the Body 1, 2, 3 and Cartesian X, Y, Z were calculated for the Tibia and Patella in the femoral coordinate system. The quadriceps force input was also tracked and RMS errors calculated between the experimental input and the control plant input to the model. Tibia RMS errors and normalized errors are



shown in Table 15, patella RMS errors and normalized errors are shown in Table 16, and the quadriceps error and normalized error is shown in Table 17.

**Table 15: Tibia RMS Error**

Run	Tibia											
	Body1	Body 1 (normalized)	Body2	Body 2 (normalized)	Body 3	Body 3 (normalized)	X	X (normalized)	Y	Y (normalized)	Z	Z (normalized)
1	4.67	0.56	4.32	0.43	28.67	0.99	45.94	0.79	9.85	0.73	9.60	0.77
2	3.50	0.42	4.02	0.40	28.65	0.99	36.73	0.63	10.54	0.78	10.07	0.81
3	3.05	0.37	3.39	0.34	28.85	1.00	34.76	0.60	10.46	0.78	10.69	0.86
4	6.67	0.80	7.03	0.71	28.00	0.97	54.86	0.94	11.34	0.84	8.75	0.70
5	6.10	0.73	6.12	0.61	28.18	0.98	52.10	0.89	11.08	0.82	8.24	0.66
6	5.05	0.61	4.82	0.48	28.39	0.98	47.60	0.82	10.31	0.77	9.35	0.75
7	8.31	1.00	9.97	1.00	27.12	0.94	58.28	1.00	13.47	1.00	12.49	1.00
8	7.87	0.95	9.51	0.95	27.36	0.95	56.76	0.97	13.06	0.97	11.38	0.91
9	6.80	0.82	7.45	0.75	27.69	0.96	55.54	0.95	11.56	0.86	9.71	0.78
10	2.66	0.32	1.70	0.17	13.96	0.48	7.75	0.13	3.31	0.25	8.90	0.71
11	2.54	0.31	1.67	0.17	13.81	0.48	7.53	0.13	3.06	0.23	8.35	0.67
12	2.53	0.30	1.64	0.16	13.74	0.48	7.34	0.13	3.04	0.23	7.85	0.63
13	2.73	0.33	1.83	0.18	14.06	0.49	8.19	0.14	3.37	0.25	9.77	0.78
14	2.71	0.33	1.78	0.18	13.88	0.48	7.80	0.13	3.27	0.24	9.31	0.74
15	2.69	0.32	1.76	0.18	13.72	0.48	7.56	0.13	3.20	0.24	8.94	0.72
16	2.81	0.34	1.84	0.18	14.51	0.50	8.32	0.14	3.73	0.28	10.19	0.82
17	2.86	0.34	1.88	0.19	14.05	0.49	8.14	0.14	3.59	0.27	9.89	0.79
18	2.75	0.33	1.85	0.19	13.81	0.48	8.01	0.14	3.23	0.24	9.60	0.77
19	2.25	0.27	2.14	0.21	12.61	0.44	8.19	0.14	4.85	0.36	5.90	0.47
20	2.25	0.27	2.14	0.22	12.58	0.44	8.30	0.14	4.85	0.36	5.90	0.47
21	2.22	0.27	2.14	0.21	12.68	0.44	8.23	0.14	5.02	0.37	5.91	0.47
22	2.22	0.27	2.08	0.21	12.64	0.44	8.23	0.14	4.74	0.35	5.99	0.48
23	2.21	0.27	2.08	0.21	12.67	0.44	8.28	0.14	4.82	0.36	6.00	0.48
24	2.20	0.26	2.09	0.21	12.67	0.44	8.47	0.15	4.89	0.36	5.99	0.48
25	2.21	0.27	2.06	0.21	12.68	0.44	8.40	0.14	4.67	0.35	6.09	0.49
26	2.19	0.26	2.05	0.21	12.69	0.44	8.36	0.14	4.75	0.35	6.08	0.49
27	2.17	0.26	2.05	0.21	12.75	0.44	8.39	0.14	4.83	0.36	6.09	0.49

**Table 16: Patella RMS Error**

Run	Patella											
	Body1	Body 1 (normalized)	Body2	Body 2 (normalized)	Body 3	Body 3 (normalized)	X	X (normalized)	Y	Y (normalized)	Z	Z (normalized)
1	6.13	0.38	4.31	0.27	17.52	0.69	4.29	0.61	6.64	0.30	10.46	0.62
2	8.10	0.51	5.52	0.35	20.97	0.82	4.30	0.61	5.89	0.26	8.84	0.52
3	8.27	0.52	5.71	0.36	21.45	0.84	4.54	0.64	5.41	0.24	8.81	0.52
4	7.33	0.46	3.83	0.24	17.07	0.67	6.31	0.89	8.35	0.37	11.62	0.69
5	6.32	0.39	3.89	0.25	16.33	0.64	5.13	0.73	8.05	0.36	11.14	0.66
6	6.22	0.39	4.33	0.27	17.06	0.67	4.67	0.66	7.06	0.31	10.80	0.64
7	16.03	1.00	15.75	1.00	25.37	0.99	5.31	0.75	22.45	1.00	16.94	1.00
8	15.68	0.98	15.43	0.98	25.57	1.00	5.15	0.73	21.90	0.98	16.84	0.99
9	8.28	0.52	3.96	0.25	18.17	0.71	7.06	1.00	8.32	0.37	12.06	0.71
10	5.16	0.32	3.56	0.23	18.18	0.71	4.63	0.66	4.61	0.21	11.38	0.67
11	4.97	0.31	3.51	0.22	18.04	0.71	4.70	0.67	4.56	0.20	11.55	0.68
12	4.78	0.30	3.56	0.23	18.47	0.72	4.87	0.69	4.02	0.18	11.93	0.70
13	5.15	0.32	3.54	0.22	18.17	0.71	4.64	0.66	4.67	0.21	11.12	0.66
14	5.22	0.33	3.55	0.23	18.21	0.71	4.57	0.65	4.67	0.21	11.25	0.66
15	4.88	0.30	3.43	0.22	17.94	0.70	4.66	0.66	4.64	0.21	11.40	0.67
16	5.64	0.35	3.80	0.24	19.22	0.75	4.70	0.67	4.15	0.18	11.23	0.66
17	5.41	0.34	3.60	0.23	18.35	0.72	4.47	0.63	4.74	0.21	11.09	0.65
18	5.26	0.33	3.53	0.22	18.23	0.71	4.47	0.63	4.71	0.21	11.18	0.66
19	3.49	0.22	3.19	0.20	18.14	0.71	5.19	0.74	6.10	0.27	16.14	0.95
20	3.46	0.22	3.18	0.20	18.11	0.71	5.17	0.73	6.09	0.27	16.13	0.95
21	3.54	0.22	3.20	0.20	18.22	0.71	5.24	0.74	6.28	0.28	16.40	0.97
22	3.45	0.22	3.28	0.21	18.13	0.71	4.98	0.71	5.18	0.23	14.83	0.88
23	3.55	0.22	3.30	0.21	18.26	0.71	4.99	0.71	5.23	0.23	14.95	0.88
24	3.51	0.22	3.29	0.21	18.24	0.71	4.98	0.71	5.28	0.24	15.05	0.89
25	3.66	0.23	3.35	0.21	18.22	0.71	4.84	0.69	4.72	0.21	14.11	0.83
26	3.75	0.23	3.37	0.21	18.35	0.72	4.86	0.69	4.77	0.21	14.22	0.84
27	4.06	0.25	3.44	0.22	18.65	0.73	4.88	0.69	4.83	0.22	14.36	0.85

**Table 17: Quadriceps Force RMS Error**

Machine Data		
Run	RMS error	RMS error (normalized)
1	410.65	0.34
2	422.06	0.35
3	411.54	0.34
4	460.90	0.38
5	474.04	0.39
6	430.55	0.35
7	596.86	0.49
8	605.87	0.50
9	432.37	0.36
10	266.77	0.22
11	288.53	0.24
12	316.53	0.26
13	249.35	0.21
14	254.88	0.21
15	262.57	0.22
16	240.25	0.20
17	245.74	0.20
18	251.23	0.21
19	1143.81	0.94
20	1141.78	0.94
21	1214.95	1.00
22	750.68	0.62
23	772.28	0.64
24	794.26	0.65
25	548.32	0.45
26	565.17	0.47
27	585.26	0.48

Different optimization profiles were run, giving different weight to each type of error, tibia error, patella error, and machine input error. The different profiles run are shown in the

tables below. Significant effects are highlighted in yellow. The results shown are shown for each factor based on the percentage of the experimental laxity test for  $L_0$ , and of the published data for  $k$  and  $\varepsilon_l$ . Profile 1 has a weighting of 2 on the tibia error and a weighting of one on the patella error and machine error. Profile 2 has a weighting of 2 on the tibia error, 0 on the patella error, and 1 on the machine error. Profile 3 has a weighting of 0 on the tibia error and patella error and a weighting of 1 on the machine error. Profile 4 has a weighting of 1 on the tibia error and a weighting of 0 on the patella error and the machine error. Profile 5 has a weighting of 0 on the tibia error, a weighting of 1 on the patella error, and a weighting of 0 on the machine error. Profile 6 has a weighting of 1 on the tibia error, the patella error, and the machine error. Profile 7 has a weighting of 1 on the tibia error, 0 on the patella error, and 2 on the machine error.

**Table 18: Profile 1: Significant Effects Highlighted in Yellow**

	B <sub>0</sub>	B <sub>1</sub>	B <sub>2</sub>	B <sub>3</sub>	B <sub>4</sub>	B <sub>5</sub>	B <sub>6</sub>	B <sub>7</sub>	B <sub>8</sub>	B <sub>9</sub>	Results	
Profile 1	8.00	2.55	-0.74	0.38	-2.47	0.64	-0.43	4.95	0.93	-0.17	Factor	%
MSE	0.57										L <sub>0</sub>	-56.82
S <sub>bk</sub> <sup>2</sup>	0.15	0.03	0.06	0.03	0.06	0.05	0.06	0.10	0.17	0.10	k	196.02
T <sub>0</sub>	20.72	14.20	-3.13	2.12	-9.92	2.92	-1.73	16.01	2.24	-0.56	ε <sub>l</sub>	79.61

**Table 19: Profile 2: Significant Effects Highlighted in Yellow**

	B <sub>0</sub>	B <sub>1</sub>	B <sub>2</sub>	B <sub>3</sub>	B <sub>4</sub>	B <sub>5</sub>	B <sub>6</sub>	B <sub>7</sub>	B <sub>8</sub>	B <sub>9</sub>	Results	
Profile 2	5.35	2.15	-0.28	0.24	-1.88	0.44	-0.20	4.40	0.43	-0.07	Factor	%
MSE	0.09										L <sub>0</sub>	-17.72
S <sub>bk</sub> <sup>2</sup>	0.02	0.01	0.01	0.01	0.01	0.01	0.01	0.02	0.03	0.02	k	153.61
T <sub>0</sub>	34.64	29.85	-2.93	3.29	-18.87	4.97	-1.98	35.50	2.62	-0.58	ε <sub>l</sub>	88.28

**Table 20: Profile 3: Significant Effects Highlighted in Yellow**

	B <sub>0</sub>	B <sub>1</sub>	B <sub>2</sub>	B <sub>3</sub>	B <sub>4</sub>	B <sub>5</sub>	B <sub>6</sub>	B <sub>7</sub>	B <sub>8</sub>	B <sub>9</sub>	Results	
Profile 3	0.20	-0.14	0.07	0.00	-0.17	0.02	-0.02	0.32	0.03	-0.01	Factor	%
MSE	0.00										L <sub>0</sub>	80.50
S <sub>bk</sub> <sup>2</sup>	0.00	0.00	0.00	0.00	0.00	0.00	0.00	0.00	0.00	0.00	k	99.71
T <sub>0</sub>	8.66	-12.65	5.13	0.01	-11.63	1.82	-1.24	17.43	1.41	-0.43	ε <sub>l</sub>	100.00

**Table 21: Profile 4: Significant Effects Highlighted in Yellow**

	B <sub>0</sub>	B <sub>1</sub>	B <sub>2</sub>	B <sub>3</sub>	B <sub>4</sub>	B <sub>5</sub>	B <sub>6</sub>	B <sub>7</sub>	B <sub>8</sub>	B <sub>9</sub>	Results	
Profile 4	2.08	1.48	-0.35	0.12	-0.42	0.15	-0.04	1.24	0.11	-0.01	Factor	%
MSE	0.03										L <sub>0</sub>	60.82
S <sub>bk</sub> <sup>2</sup>	0.01	0.00	0.00	0.00	0.00	0.00	0.00	0.00	0.01	0.00	k	107.86
T <sub>0</sub>	25.30	38.63	-7.04	3.08	-8.00	3.15	-0.82	18.78	1.28	-0.18	ε <sub>l</sub>	97.28

**Table 22: Profile 5: Significant Effects Highlighted in Yellow**

	B <sub>0</sub>	B <sub>1</sub>	B <sub>2</sub>	B <sub>3</sub>	B <sub>4</sub>	B <sub>5</sub>	B <sub>6</sub>	B <sub>7</sub>	B <sub>8</sub>	B <sub>9</sub>	Results	
Profile 5	2.64	0.40	-0.46	0.14	-0.59	0.20	-0.23	0.55	0.49	-0.10	Factor	%
MSE	0.23										L <sub>0</sub>	76.41
S <sub>bk</sub> <sup>2</sup>	0.06	0.01	0.02	0.01	0.02	0.02	0.02	0.04	0.07	0.04	k	102.96
T <sub>0</sub>	10.80	3.54	-3.09	1.26	-3.72	1.46	-1.48	2.82	1.88	-0.51	ε <sub>l</sub>	100.00

**Table 23: Profile 6: Significant Effects Highlighted in Yellow**

	B <sub>0</sub>	B <sub>1</sub>	B <sub>2</sub>	B <sub>3</sub>	B <sub>4</sub>	B <sub>5</sub>	B <sub>6</sub>	B <sub>7</sub>	B <sub>8</sub>	B <sub>9</sub>	Results	
Profile 6	5.91	1.07	-0.39	0.26	-2.05	0.49	-0.39	3.71	0.81	-0.16	Factor	%
MSE	0.40										L <sub>0</sub>	40.17
S <sub>bk</sub> <sup>2</sup>	0.10	0.02	0.04	0.02	0.04	0.03	0.04	0.07	0.12	0.07	k	127.44
T <sub>0</sub>	18.27	7.11	-1.95	1.74	-9.79	2.68	-1.85	14.31	2.34	-0.62	ε <sub>l</sub>	93.40

**Table 24: Profile 7: Significant Effects Highlighted in Yellow**

	B <sub>0</sub>	B <sub>1</sub>	B <sub>2</sub>	B <sub>3</sub>	B <sub>4</sub>	B <sub>5</sub>	B <sub>6</sub>	B <sub>7</sub>	B <sub>8</sub>	B <sub>9</sub>	Results	
Profile 7	4.46	-0.14	0.51	0.12	-2.49	0.43	-0.26	5.08	0.53	-0.11	Factor	%
MSE	3.72										L <sub>0</sub>	80.00
S <sub>bk</sub> <sup>2</sup>	0.97	0.21	0.36	0.21	0.40	0.31	0.40	0.62	1.11	0.62	k	100.00
T <sub>0</sub>	4.54	-0.31	0.85	0.26	-3.93	0.77	-0.42	6.45	0.50	-0.14	ε <sub>l</sub>	100.00

## CHAPTER 5

### CONCLUSION

The optimization profiles present many different conclusions. Each profile must be evaluated to determine the usefulness of its results. Many factors can effect whether or not the results are useful. The results must be within a realistic range, and must not put the knee through impossible motions or put the ligaments past their yield strength. Profile 1 and profile 2 fail to produce results that are possible. Both profiles produce negative zero load lengths, which would cause the ligaments to be in tension no matter the situation, since bone cannot pass through bone. This is in contradiction to published findings that the ACL should show maximum strain at  $10^{\circ}$  of flexion and should go slack when the knee is flexed  $>17^{\circ}$  (Pope et al., 1991) and is loaded throughout the stance phase of gait (Shelburne et al., 2005). The PCL was not loaded during the stance phase, the MCL was not loaded much during the stance phase and the LCL was only loaded just before the contralateral toe-off and before the contralateral heel-strike during normal walking (Shelburne et al., 2005). In profile 4, the force on the ACL at the beginning of the gait cycle is 2159 N on the aACL and 2342 N on the pACL. The average failure strength of the ACL according to Stapleton et al., 1998 is 2362.5 N, implying that the ACL starts the simulation dangerously close to failure. In profile 6, the aACL starts the simulation at 7242 N and the pACL starts at 7568 N, which is approximately 3 times the average failure strength of the ACL. Both profile 4 and 6 present situations which are obviously not possible, since the experimental knee performed the simulation intact. Profiles 3, 5 and 7 result in situations where the ligaments experience tension values that are within a normal range. Further, the resulting  $k$  values match closely with publish values.



From profiles 3, 5 and 7, it can be concluded that the zero load length ( $L_0$ ) should be between 75% and 80% of experimentally derived values. The stiffness ( $k$ ) of the ligaments should be set to published values, as the profiles range from 99.71% to 102.96% of published values. Last the value of  $\varepsilon_l$  is not significant to the prediction equations in these profiles, indicating that its value is not important to the simulation. Therefore, using the published value of  $\varepsilon_l$  is appropriate for knee simulation models.

## CHAPTER 6

### DISCUSSION

The model of the specimen knee in the KKS reproduces tibia and patella kinematics with reasonable accuracy. The optimization techniques used provide different approximations of the ligament properties. Optimization based on machine input RMS error and patellofemoral RMS error provide reasonable approximations of the ligament properties, while the optimization schemes based on tibiofemoral RMS error provide unreasonable approximations of the ligament properties.

#### Tibiofemoral Optimization

Tibiofemoral optimization provided unreasonable results. At high values of ligament stiffness ( $k$ ) and low values of zero load length ( $L_0$ ), the machine control plant raises the input force of the quadriceps force, in order to match the hip angle. The increase in the quadriceps force compensates for the error that would otherwise occur in the tibia marker relative to the femoral marker. If the PID control plant were replaced with a direct input, it is believed that higher tibiofemoral RMS errors would occur. Further modeling work would be needed to verify the results of tibiofemoral optimization with a direct input control method.

#### Patellofemoral Optimization

Unlike the tibiofemoral optimization, the patellofemoral optimization provides reasonable results. When the quadriceps force is increased to compensate for the hip angle, the quadriceps tendon and the patellar tendon stretch, pulling the patella out of place when compared to experimental results. This can be observed mainly in the patella Z RMS error. As the machine RMS error increases, due to the PID control plant, the patella Z RMS error also increases.

### Machine RMS Optimization

The machine RMS error is based on the quadriceps force. As changes are made to the model, the PID control plant attempts to match the hip angle of the experimental results by modifying the quadriceps input force. The most significant values of the machine RMS error are found when  $k$  is at a high value and  $L_0$  is at a low value. In this situation, the preload on the ligaments is the highest. Therefore, the knee requires significantly more force from the quadriceps to move when compared to experimental results.

### Future Work

The work done here provides a basis for understanding ligament modeling techniques for subject specific knee models. There is much work that can be done to validate the results. These techniques need to be tested on more subject knees and comparisons need to be made between models with and without a PID control plant. Further, ligament optimization should be tested on individual ligaments, as opposed to the entire system as a whole.

An important step to validating the results is to research optimization of different subject knees. This would provide important information about whether these results are universal for subject specific knees, or whether each knee requires an individual optimization. Future work would not require inclusion of  $\varepsilon_l$ , as it proved insignificant for all model configurations, reducing the number of runs from 27 to 9.

Further, if the optimization techniques were applied to a knee with a direct input control plant, it is believed that the tibiofemoral RMS errors would prove more useful to optimization, while eliminating the need to track machine input RMS error. Because the direct input control plant would not allow for machine compensation, the knee would not be able to move under the experimental loads with significantly increased ligament preloads. Comparisons between the

PID control models and direct input control models would show any discrepancies, and provide useful information on the advantages or disadvantages of both systems.

Last, more research needs to be done on the individual ligaments. Optimization in this study was accomplished by testing all of the ligaments in the system in the same state. Treating the ligaments as separate could provide information on whether all the ligaments are optimized at the same values, or whether they each have different values.

## Appendix

Lig\_lenth\_crunch.m:

%1/16/2008

%Kevin Dodd

%Lig\_length\_crunch.m

%

%This program is used to convert the transformation matrix of the

%rigid bodies in the Optotrak frame into anatomical kinematics in the

%femoral frame. It also includes code that will find the distance between

%two points during the activity, such as the distance of the insertion and

%origon of a ligament or some other points of intrest on the tibia or

%patella relative to a point on the femur.

%

%This program calls several other programs and requires differnt data in

%the raw form. A discription of the Data and the Programs are listed.

%=====

%Required programs

%    mechaxis.m    Transformation of the Femur, Tibia and Patella axis

%                   relative to GS anatomical points

%    GS\_lig.m      The conversion of raw data into GS kinematic

%                   description

%    distance.m    Finds the distance between two points on moving

%                   bodies

%=====

%Required data

% Raw optotrak kinematics

% Anatomical point file

% KKS probed points or VV correction angle

% Insertion matrix (Tibia Frame)

% Origin matrix (Femoral Frame)

%NOTE: The order of the file content are important on the point files. The  
%anatomical and KKS probed points should be as they were given in each  
%respective file (NK0X\NK0XR\_Opto\NK0XR\_kinematics). This is how the  
%original Kinematics were run. The correction VV was calculated using the  
%KKS points. Please note that the files can be changed to points probed on  
%the model but the order must remain the same.

%

%The correction angle used for the NK01-NK06 are as follows

% NK01R 4.9

% NK02R 5.26

% NK03R 4.08

% NK04R 1.92

% NK05L -5.21

% NK06L -7.51

%=====

%OUTPUT FILES

%The Output file will contain an [n X m] matrix. "m" will vary depending  
%on how many points are being analysed. The first 13 columns are the GS

```

%kinematic description of the tibia and patella motion. The next columns
%are the ligament lengths at that time step. The order of the ligmant
%columns are the same as the order of the Insertion and Origin files.
%
%=====
=====

%Variables
%    Env
%    GSpt
%    ang
%    TRb_f
%    TRb_t
%    TRb_p

clear

clc

warning off

%Read in the 6d envelope file (Must be changed to accomodate correct file path)
%Use all envelope kinematic data if possible.

Env1=xlsread('Raw_Envelope\NK02R_env_nat_1_Raw.csv');
Env2=xlsread('Raw_Envelope\NK02R_env_nat_2_Raw.csv');
Env3=xlsread('Raw_Envelope\NK02R_env_nat_3_trent_Raw.csv');
Env=[Env1;Env2;Env3];

```

```

%read in the anatomical point files

GSpt=dlmread('Anatomical points\NK02R_Anat.txt');

%Find the transformation matrix of the femur, tibia, and patella to its
%respective rigid body.

a=5.26;

[ang,TRf_f,TRt_t,TRp_p]=mech_axis(GSpt,a);


%Read in the ligament point files

Insert=dlmread('Ligament Attachment\NK02R_tib_lig_attach.txt');
Origin=dlmread('Ligament Attachment\NK02R_fem_lig_attach.txt');

In=[mean(Insert(31:40,:));
    mean(Insert(21:30,:));
    mean(Insert(1:10,:));
    mean(Insert(11:20,:))];

O=[mean(Origin(31:40,:)); %Magenta
   mean(Origin(21:30,:)); %Green
   mean(Origin(1:10,:)); %Yellow ACL
   mean(Origin(11:20,:))]; %Red PCL


Env_lig=GS_lig(GSpt,Env,TRf_f,TRt_t,TRp_p,In,O);

rbg=hsv(size(In,1));

```



```
figure(1)
hold on
for m=1:size(Env_lig,2)-13;

    plot(Env_lig(:,1),Env_lig(:,m+12),'.','color',rbg(m,:))
    xlabel('Flexion');ylabel('Lig I/O dist')
    axis([-20 150 0 140]);
end
```

## REFERENCES

- Abdel-Rahman, E. M. and M. S. Hefzy. Three-dimensional dynamic behavior of the human knee joint under impact loading. *Medical Engineering & Physics* 20, no. 4 (1998): 276-90.
- Bertozzi L, Stagni R, Fantozzi S and Cappello A. Evaluation of a cruciate ligament model: sensitivity to the parameters during drawer test simulation. *Journal of Applied Biomechanics*, 24 (2008):234-243.
- Blankevoort, L., J. H. Kuiper, R. Huiskes, and H. J. Grootenboer. Articular contact in a three-dimensional model of the knee. *Journal of Biomechanics* 24, no. 11 (1991): 1019-031.
- Butler D. L., M. D. Kay, D. C. Stouffer. Comparison of material properties in fascicle-bone units from human patellar tendon and knee ligaments. *Journal of Biomechanics* 19, no. 6 (1986):425-32.
- Caruntu, D. I. and M. S. Hefzy. 3-d anatomically based dynamic modeling of the human knee to include tibio-femoral and patello-femoral joints. *Journal of Biomechanical Engineering* 126, no. 1 (2004): 44-53.
- Chhabra, Anikar, James S. Starman, Mario Ferretti, Armando F. Vidal, Thore Zantop, and Freddie H. Fu. Anatomic, radiographic, biomechanical, and kinematic evaluation of the anterior cruciate ligament and its two functional bundles. *The Journal of Bone and Joint Surgery* 88-A.4 (2006): 2-10.
- DeFrate, Louis E., Thomas J. Gill, and Guoan Li. In Vivo function of the posterior cruciate ligament during weightbearing knee flexion. *The American Journal of Sports Medicine* 32, no. 8 (2004): 1923-928.
- Guess, T. M. and L. P. Maletsky. Computational modelling of a total knee prosthetic loaded in a dynamic knee simulator. *Medical Engineering and Physics* 27, no. 5 (2004): 357-367.
- Lyman S, Koulouvaris P, Sherman S, Do H, Mandl LA, Marx RG. Epidemiology of anterior cruciate ligament reconstruction: trends, readmissions, and subsequent knee surgery. *Journal of Bone and Joint Surgery* 91, no. 10 (Oct 2009):2321-8.
- Park, Sang Eun, Louis E. DeFrate, Jeremy F. Suggs, Thomas J. Gill, Harry E. Rubash, and Guoan Li. Erratum to The change in length of the medial and lateral collateral ligaments during in vivo knee flexion. *The Knee* 13 (2006): 77-82.
- Piazza and Delp. Three-dimensional dynamic simulation of total knee replacement motion during a step-up task. *Journal of Biomechanical Engineering* 123, no. 6 (2001): 599-606.
- Pope, M.H., C.J. Stankewich, B.D. Beynnon, and B.C. Fleming. Effect of knee musculature on anterior cruciate ligament strain in vivo. *Journal of Electromyography and Kinesiology* 1, no. 3 (1991): 191-98.

- Rekab, Kamel, and Muzaffar Shaikh. *Statistical Design of Experiments with Engineering Applications (Statistics: a Series of Textbooks and Monographs)*. Null: CRC, 2005.
- Shelburne, Kevin B., Michael R. Torry, and Marcus G. Pandy. Muscle, ligament, and joint-contact forces at the knee during walking. *Medicine & Science in Sports & Exercise* 37, no. 11 (2005): 1948-956.
- Stapleton, Timothy R., John I. Waldrop, Craig R. Ruder, Todd A. Parrish, and Thomas E. Kuivila. Graft fixation strength with arthroscopic anterior cruciate ligament reconstruction two-incision rear entry technique compared with one-incision technique. *The American Journal of Sports Medicine* 26, no. 3 (1998): 442-45.
- Weimer, Katherine. *Development and Validation of a Subject-Specific Computational Human Knee Model in a Dynamic Knee Simulator to Include Ligament and Tendon Bone Wrapping* Thesis. University of Missouri - Kansas City, 2006.
- Weiss, Jeffrey A., and John C. Gardiner. Computational modeling of ligament mechanics. *Critical Reviews in Biomedical Engineering* 29, no. 4 (2001): 1-70.

## VITA

Paul Michael Wilson was born on August 13, 1981, in Kansas City, Missouri. He was educated in local public schools, until moving to Gainesville, Florida, where he graduated from Gainesville High School in 2000. He received an academic scholarship from the state of Florida as part of the Bright Futures program, and started attending University of Florida in the mechanical engineering program. In 2004, Paul transferred to University of Missouri – Kansas City.

He continued studying mechanical engineering at University of Missouri – Kansas City, and also served as treasurer of the School of Computing Student Council, President of Tau Beta Pi, and President of Pi Tau Sigma, and Team Captain of the Human Powered Vehicle Design Team. He was a teaching assistant for Instruments and Measurements Lab I and II his senior year, and graduated summa cum laude in 2007 to complete his Bachelor of Science Degree in Mechanical Engineering.

Fall 2007 he enrolled in the University of Missouri – Kansas City Graduate School and assumed a position as a graduate teaching assistant for Instruments and Measurements Lab I and II. Fall 2009 He assumed a graduated research assistant position in the Musculoskeletal Biomechanics Research Laboratory. Upon completion of his Masters of Science in Mechanical Engineering, Paul plans to use his education to follow a career in engineering.